3-2024

Nonlinear Interactions of Sea-Level Rise and Storm Tide Alter Extreme Coastal Water Levels: How and Why?

H. Moftakhari
University Of Alabama

D. F. Muñoz
University of Alabama

A. Akbari Asanjan
Universities Space Research Association

A. AghaKouchak
University of Alabama

Hamid Moradkhani
University of Alabama

See next page for additional authors

Citation Details

Moftakhari, H., Muñoz, D. F., Akbari Asanjan, A., AghaKouchak, A., Moradkhani, H., & Jay, D. A. (2024). Nonlinear Interactions of Sea-Level Rise and Storm Tide Alter Extreme Coastal Water Levels: How and Why?. AGU Advances, 5(2), e2023AV000996.

AGU ADVANCING EARTH AND SPACE SCIENCES

AGU Advances

RESEARCH ARTICLE
10.1029/2023AV000996

Nonlinear Interactions of Sea-Level Rise and Storm Tide Alter Extreme Coastal Water Levels: How and Why?

H. Moftakhari[1,2], D. F. Muñoz[1,2,3], A. Akbari Asanjan[4,5], A. AghaKouchak[6,7], H. Moradkhani[1,2], and D. A. Jay[8]

[1]Center for Complex Hydrosystems Research, The University of Alabama, Tuscaloosa, AL, USA, [2]Department of Civil, Construction and Environmental Engineering, The University of Alabama, Tuscaloosa, AL, USA, [3]Department of Civil, and Environmental Engineering, Virginia Tech, Blacksburg, VA, USA, [4]Universities Space Research Association, Washington, DC, USA, [5]NASA Ames Research Center, Mountain View, CA, USA, [6]Department of Civil and Environmental Engineering, University of California, Irvine, Irvine, CA, USA, [7]Department of Earth System Science, University of California, Irvine, Irvine, CA, USA, [8]Department of Civil and Environmental Engineering, Portland State University, Portland, OR, USA

Peer Review The peer review history for this article is available as a PDF in the Supporting Information.

Key Points:

- We use global hourly tidal data to show how and why tides and surges interact with mean sea level (MSL) fluctuations
- In 37% of studied locations, Potential Maximum Storm Tide (PMST), a proxy for Extreme coastal water level, co-varies with MSL
- Sea-level rise and MSL-storm tide interactions are captured by PMST statistics and contribute to the estimated increase in flood hazard at 75% of locations by 2050

Supporting Information:

Supporting Information may be found in the online version of this article.

Correspondence to:

H. Moftakhari,
hmoftakhari@ua.edu

Citation:

Moftakhari, H., Muñoz, D. F., Akbari Asanjan, A., AghaKouchak, A., Moradkhani, H., & Jay, D. A. (2024). Nonlinear interactions of sea-level rise and storm tide alter extreme coastal water levels: How and why? *AGU Advances*, *5*, e2023AV000996. https://doi.org/10.1029/2023AV000996

Received 11 JULY 2023
Accepted 10 FEB 2024

Author Contributions:

Conceptualization: H. Moftakhari, D. A. Jay
Data curation: H. Moftakhari, D. F. Muñoz
Formal analysis: H. Moftakhari, D. F. Muñoz
Funding acquisition: H. Moftakhari, D. F. Muñoz, H. Moradkhani
Investigation: H. Moftakhari
Methodology: H. Moftakhari, A. Akbari Asanjan, A. AghaKouchak, H. Moradkhani, D. A. Jay

Abstract Sea-level rise (SLR) increasingly threatens coastal communities around the world. However, not all coastal communities are equally threatened, and realistic estimation of hazard is difficult. Understanding SLR impacts on extreme sea level is challenging due to interactions between multiple tidal and non-tidal flood drivers. We here use global hourly tidal data to show how and why tides and surges interact with mean sea level (MSL) fluctuations. At most locations around the world, the amplitude of at least one tidal constituent and/or amplitude of non-tidal residual have changed in response to MSL variation over the past few decades. In 37% of studied locations, "Potential Maximum Storm Tide" (PMST), a proxy for extreme sea level dynamics, co-varies with MSL variations. Over all stations, the median PMST will be 20% larger by the mid-century, and conventional approaches that simply shift the current storm tide regime up at the rate of projected SLR may underestimate the flooding hazard at these locations by up to a factor of four. Micro- and meso-tidal systems and those with diurnal tidal regime are generally more susceptible to altered MSL than other categories. The nonlinear interactions of MSL and storm tide captured in PMST statistics contribute, along with projected SLR, to the estimated increase in flood hazard at three-fourth of studied locations by mid-21st century. PMST is a threshold that captures nonlinear interactions between extreme sea level components and their co-evolution over time. Thus, use of this statistic can help direct assessment and design of critical coastal infrastructure.

Plain Language Summary Sea-level rise poses a significant threat to coastal communities worldwide, but the level of risk varies across different areas, making accurate estimation challenging. This study analyzed the tidal data from around the Globe to understand the complex interactions between tides, surges, and mean sea level (MSL) fluctuations. The research found that in most locations, tides and non-tidal residuals have changed due to variations in MSL over recent decades. This research proposes a conservative proxy for extreme sea level dynamics, called "Potential Maximum Surge Tide" (PMST). By mid-century, the median PMST is projected to be 20% higher over all monitoring stations. Simply shifting storm tide predictions up based on projected SLR may underestimate the flooding risk up to fourfold. The interactions between MSL and storm tides, captured through the PMST statistic, contribute to increased flood hazards at three-quarters of the studied locations by the mid-21st century. Thus, information provided via PMST statistics can guide the design and assessment of important coastal infrastructure, and enhance preparedness for future flood risks.

1. Introduction

Sea-level rise (SLR) is accelerating, and given the current trajectory of warming, a rise in global mean sea-level exceeding 1 m is possible during the 21st century (Dangendorf et al., 2019; IPCC, 2019; Palmer et al., 2020). This rise reduces the freeboard between high tidal datum and flood stage, which introduces uncertainties in flood risk allowances that need to be considered in coastal risk and adaptation assessments (Arns et al., 2017; Boumis et al., 2023a; Buchanan et al., 2016; Hunter, 2012; Nicholls et al., 2021). Currently, 250 million people live on a land below annual coastal flood levels; without protective measures; this number may reach 340 million by 2050 (Kulp & Strauss, 2019). This estimate of coastal flooding exposure is based, however, on shifting today's storm tide regime to a higher elevation for a given SLR scenario, ignoring nonlinear interactions between tidal and non-

Software: H. Moftakhari, D. F. Muñoz
Validation: H. Moftakhari, D. A. Jay
Visualization: H. Moftakhari
Writing – original draft: H. Moftakhari, D. A. Jay
Writing – review & editing: H. Moftakhari, D. F. Muñoz, A. Akbari Asanjan, A. AghaKouchak, H. Moradkhani, D. A. Jay

tidal components of coastal water level and future mean sea levels (MSLs) (Hinkel et al., 2014; Kulp & Strauss, 2019; Neumann et al., 2015). We show that this approach under-estimates coastal flood hazard in some regions, while over-estimating it in others.

Extreme coastal water level (ECWL) is determined as the combination of MSL, harmonics tides (HT), and the non-tidal residuals (NTR). MSL refers to the arithmetic mean of hourly heights observed over a relatively long period (preferably several years). HT, is the most predictable component of ECWL (Gregory et al., 2019; Parker, 2007); it is the sum of astronomical tides and overtides (NOAA-COOPS, 2000). NTR refers to the difference between observed still water level and estimated HT thus, NTR contains both surge, driven by wind and pressure, and the tide-surge interactions (Fernández-Montblanc et al., 2019). The sum of NTR and HT is called storm tide (NOAA-COOPS, 2000); thus:

$$\text{ECWL} = \text{MSL} + \text{storm tide} = \text{MSL} + \text{HT} + \text{NTR} \quad (1)$$

The spatio-temporal variability of ECWL will change in a warming climate at global and regional scales (Calafat et al., 2022; Goodwin et al., 2017; Marcos et al., 2015; Mawdsley & Haigh, 2016; Muis et al., 2016, 2019, 2020; Rashid et al., 2019). NTR, composed of intra-annual/interannual variability and a high-frequency residual related to storm surge due to atmospheric pressure anomalies and wind setup, is expected to be altered by climate change (Serafin et al., 2017). There is ample evidence that trends in the climate factors have significantly affected wave characteristics over the past few decades and that shifts in oceanic currents will occur in a warming climate (Bromirski & Cayan, 2015; Johnson & Lyman, 2020; Melet et al., 2018; Morim et al., 2020; Semedo et al., 2011; Tebaldi et al., 2021). Moreover, altered terrestrial inflows to coastal regions will likely change NTR through quadratic bottom friction and their steric contribution to sea level (Guo et al., 2015; Hoitink & Jay, 2016; Matte et al., 2013; Xiao et al., 2021). While changes will be partially due to climate forcing (Gori et al., 2022; Marsooli et al., 2019; Wahl & Chambers, 2016), nonlinear interactions among different components of ECWL are also important (Arns et al., 2020). Further, HT characteristics (amplitudes and phases) are subject to change due to non-astronomical factors (Haigh et al., 2019; Woodworth, 2010). HTs are shallow-water waves and react to changes in MSL through barotropic effects, including frictional effects and altered tidal resonance (Talke & Jay, 2020), and a variety of internal processes (Idier et al., 2017). These MSL-HT interactions are nonlinear, and often highly variable in a single oceanic region (Devlin et al., 2014; Wahl, 2017). MSL-NTR interactions are also hard to characterize, because wind patterns may change, and SLR may either amplify the NTR via reduced friction or dampen it via reduced surface wind stress on the water column (Arns et al., 2020; De Dominicis et al., 2020; Familkhalili & Talke, 2016). NTR also interacts with HT via nonlinear phase and amplitude alterations (Proudman, 1955a; Rossiter, 1961). Thus, nonlinear HT-NTR interactions contribute to altered ECWL dynamics in a changing climate (Familkhalili et al., 2020; Idier et al., 2012) and modulate coastal flooding regime associated with ECWL (Bilskie et al., 2016, 2022; S. L. Dykstra & Dzwonkowski, 2021; S. Li et al., 2021; Rashid et al., 2021).

Historically, scientists have often failed to connect SLR with an exacerbated coastal flooding risk, for various reasons. In certain regions, MSL has actually decreased (e.g., parts of Northern Europe and the Northeast Pacific Ocean), or there has been an inconsequential/negative correlation between the fluctuation in MSL and the height of storm tides (Pickering et al., 2012, 2017; Woodworth et al., 2007). However, recent studies have explored regional patterns in MSL-HT interactions, and reported significant correlation between HT and MSL in gauges across Pacific and Atlantic oceans (Jay, 2009; Devlin et al., 2019; Devlin, Jay, Talke, et al., 2017; Devlin, Jay, Zaron, et al., 2017; D. Idier et al., 2017; Pickering et al., 2012, 2017; Ray & Talke, 2019; P.L. Woodworth, 2010), as reviewed by Jay et al. (2021). Thompson et al. (2021) studied the combined effects of SLR and nodal cycle modulations of tidal amplitude on frequency of high tide flooding around the United States, and found that there might be a rapid increase in the frequency of high tide flooding in multiple US coastal regions after mid-2030s. In freshwater-influenced systems like estuaries and bays, however, the process is more complicated, because MSL is influenced by freshwater influx from riverine tributaries as well (Hoitink & Jay, 2016; Jay et al., 2015; Khojasteh et al., 2023). In these systems, frictional interactions of the main tidal constituents with each other and with freshwater influx gives rise to the overtides and dampen tides (Guo et al., 2015; Proudman, 1955b). Thus, a higher MSL is not necessarily associated with higher flooding hazard. Moreover, time scale matters. At San Francisco, MSL and the amplitude of the largest lunar tidal constutuent M_2 have both increased over the last 160 years, but on a seasonal scale, fluctuations in MSL and M_2 are anti-correlated (Moftakhari et al., 2013; Talke & Jay, 2020).

Finally, increasing or decreasing inflow to the coast may raise or lower local steric heights (e.g., Devlin et al., 2018), thereby affecting tides.

Here, we integrate the contributions of various tidal and non-tidal components of coastal water level to flooding, using a proxy for ECWL fluctuations around MSL called Potential Maximum Storm Tide (PMST). PMST is a coastal flood hazard upper limit or threshold that captures the nonlinear dynamics between MSL, NTR and HA, and is helpful in characterizing the co-evolution of these components of ECWL with SLR. We then use hourly water level data from global tide gauges (Woodworth et al., 2016) to quantify how tidal and non-tidal components of PMST interact with MSL around the globe. PMST generally represents the highest NTR on top of a perigean spring tide (Wood, 1978), or in media jargon, a *king tide*. An extreme example occurred during Hurricane Sandy —a coincidence of a storm surge and the peak of *king tide* reached a water level significantly greater than the previous record and resulted in a "significant change" in exceedance probability calculations (W. Sweet et al., 2013; Zervas, 2013). To calculate PMST, we take the sum of amplitude for the five major diurnal and semidiurnal tidal constituents plus three overtides and the largest NTR (more details in the Methods section). The probability of PMST occurring is low, because it ignores the phase difference between tidal constituents and the lag time between NTR and greater diurnal/semidiurnal fluctuations. Nonetheless, major storms occur on king or perigean spring tides often enough to be culturally important; for example, Wood (1978) describes a considerable number of such events in North America, starting in 1635. Next, using site-specific probabilistic relative SLR projections (Kopp et al., 2014, 2017), we estimate how the nonlinear interactions among flood hazard drivers affect estimated PMST in the upcoming decades.

2. Materials and Methods

Hourly water level data from a global tide gauge set were obtained from the GESLA-2 database (Woodworth et al., 2016). We analyzed 446 sites with at least 19 years of observations, and less than 20% gaps over the entire record. Where there were multiple data files for the same station in different time periods,the files were merged to provide the longest possible record. A harmonic analysis package, *t_tide*, was used to calculate harmonic constituents (phase and amplitude) of the observed tides (Leffler & Jay, 2009; Pawlowicz et al., 2002). We applied *t_tide* using a 40-day moving window over the length of each record in steps of three days, requiring at least 98% complete data at each step. Thus, there is ~92% overlap in the time period for each estimate of MSL and HT. Only constituents with signal-to-noise ratio greater than two were used in the further analyses. Astronomically forced "nodal" variability of constituents (with 4.4, 8.8, and 19.6-yr periodicities) was accounted for using the nodal correction feature of *t_tide* (Pawlowicz et al., 2002). While the actual nodal variability at some stations departs somewhat from that estimated by *t_tide*, this approach removes most of astronomically driven constituent variability. The calculated tidal constituents for each 40-day window were then used to estimate HT over the same window. The timeseries of NTR, defined as the difference between observed water level and the estimated HT over the calculating window, was estimated as:

$$\mathrm{NTR}(\tau) = \mathrm{WL}(\tau) - \mathrm{MSL} - \mathrm{HT}(\tau) \tag{2}$$

where $\mathrm{WL}(\tau)$ is the timeseries of observed water levels over the length of a calculating window. MSL is the arithmetic average of observed water level over the 40-day window, as:

$$\mathrm{MSL} = \frac{\sum_{i=1}^{T} WL_i}{T} \tag{3}$$

and the harmonic tides are reconstructed as:

$$\mathrm{HT}(\tau) = \sum_{i=1}^{n} A_i \cos\left(\omega_i \tau - \varphi_i\right) \tag{4}$$

where, n is the number of significant constituents in harmonic analysis, and A_i,ω_i and φ_i are the amplitude, frequency and phase of constituent i. Then the largest $\mathrm{NTR}(\tau)$ over ±1 day around the central day of each window

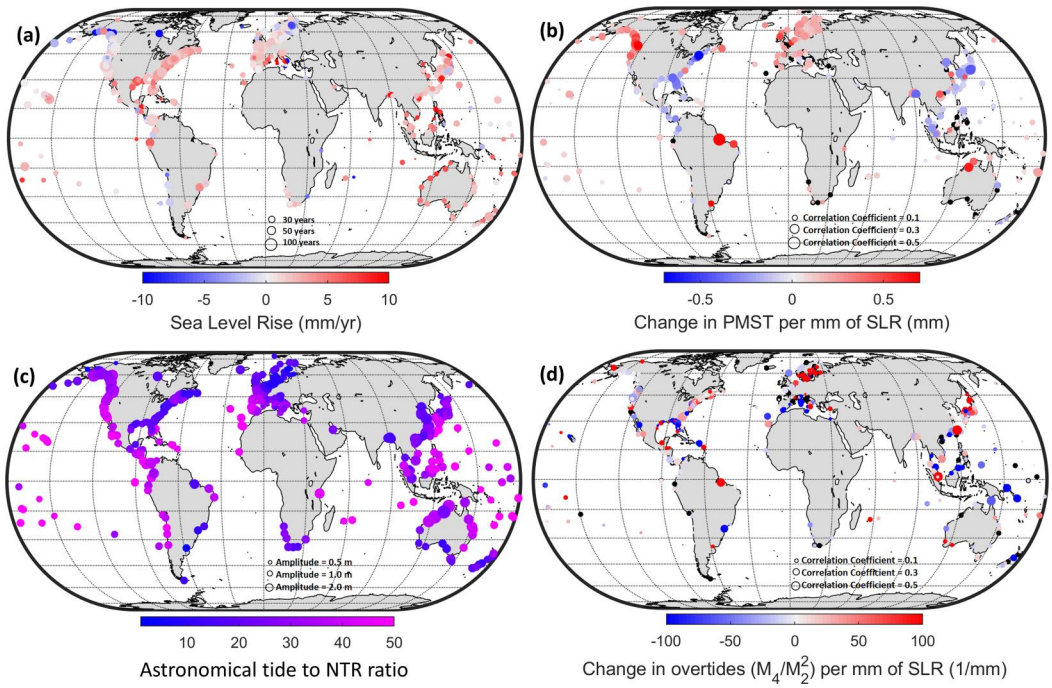

Figure 1. Observed changes in the drivers of coastal flooding. (a) rate of mean sea level (MSL) rise (size of the circle at each location represents the length of available record at that gauge); (b) rate of change in Potential Maximum Storm Tide (PMST) per millimeter (mm) change in MSL (size of the circle at each location represents the correlation coefficient (CC) between PMST and MSL); (c) average tide (harmonics tides) to non-tidal residual (non-tidal residuals) ratio (size of the circle at each location represents the average sum of amplitude for the five major tidal constituents; K_1, O_1, M_2, N_2, and S_2, and the three overtides M_4, MK_3, and MS_4); (d) rate of change in amplitude of overtides per mm change in MSL (size of the circle at each location represents the CC between M_4/M_2^2 and MSL). Black circles in panels b and d represent the points with insignificant rank correlation (p-value > 0.05).

was stored as NTR associated with that window. So while the MSL and tidal constituents are calculated over a 40-day moving window the effective temporal resolution of the PMST estimates is 3-day.

To calculate PMST, we take the sum of amplitude for the five major tidal constituents, namely main lunar diurnal (K_1 and O_1) and semidiurnal (M_2, N_2, and S_2) tides (Pugh & Woodworth, 2014) plus three important overtides (M_4, MK_3, and MS_4) calculated over a 40-day window and the largest NTR calculated over the central three days of the same calculating window, as:

$$\mathrm{PMST} = A_{\mathrm{K1}} + A_{\mathrm{O1}} + A_{\mathrm{M2}} + A_{\mathrm{N2}} + A_{\mathrm{S2}} + A_{\mathrm{M4}} + A_{\mathrm{MK3}} + A_{\mathrm{MS4}} + \mathrm{NTR} \quad (5)$$

PMST is a statistic that is broadly applicable to diverse diurnal, semidiurnal and mixed tidal regimes. It is an upper limit, and upper limits or thresholds on complex phenomena are useful in many engineering contexts (Cheung et al., 2011; Faber & Stewart, 2003; Karamouz et al., 2022; Yim et al., 2015). In this situation, we need a parameter that: (a) can be used globally, regardless of the tidal characteristics at a given location; and (b) provides a solid upper limit. PMST achieves both of these objectives, because it is an upper limit that is applicable to diverse diurnal, semidiurnal and mixed tidal regimes. While PMST linearizes complex nonlinear processes, it compensates for this in a conservative manner by adding constituent amplitudes. A simple measure of this sort is the only practical possibility for a global analysis, because there is no single pattern of MSL-HT-NTR interactions that applies even regionally (e.g., Devlin et al., 2014).

Further, PMST is not unduly conservative. To use an example particularly relevant to semidiurnal and mixed tidal regimes: it might happen only once every few centuries that a storm would occur at any given location within a few days of a perigean tide at a time when the moon is particularly close to the earth (representing an especially close conjunction of M_2, S_2, N_2, and their overtides). But it is not at all improbable that a major storm will occur somewhere on earth in a semidiurnal tidal regime within a few days of this event. An example of this is the "Saxby

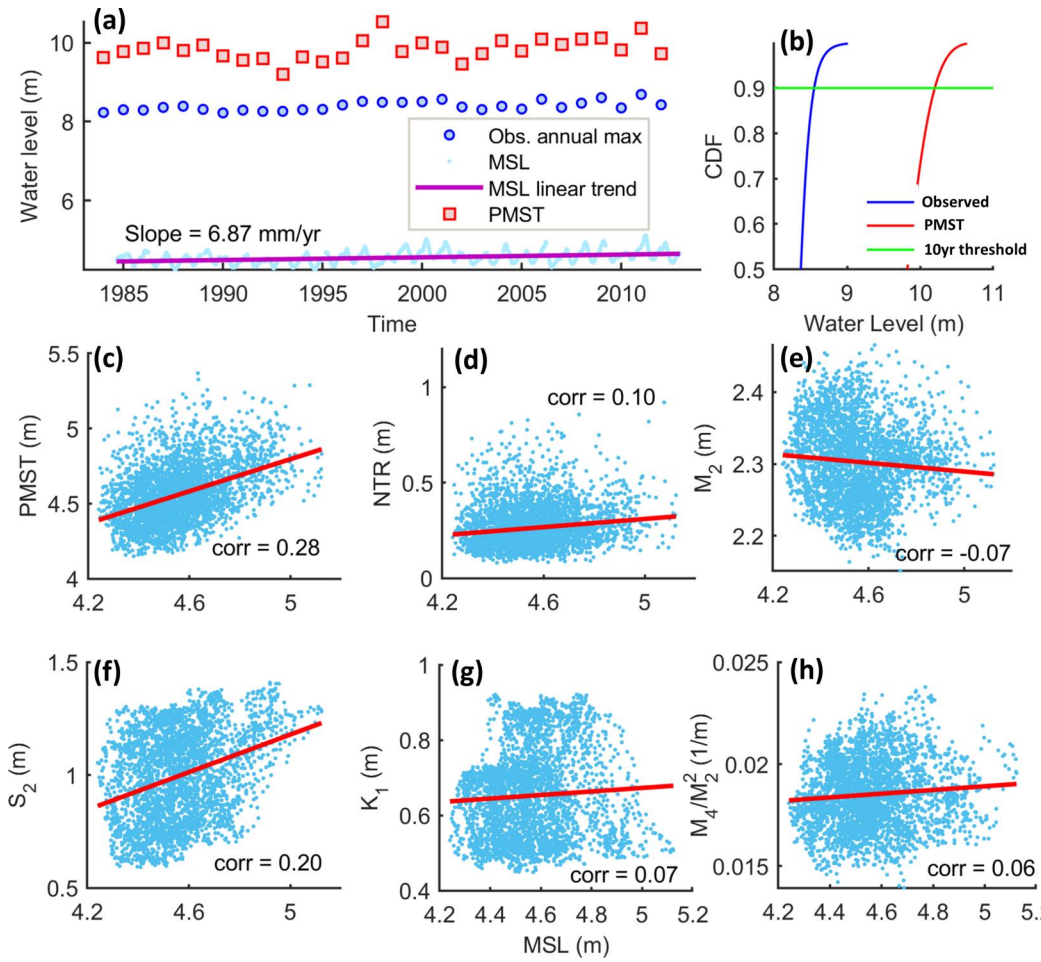

Figure 2. Trends and relationships at Wyndham, Australia. (a) Historic trends in mean sea level (MSL) and observed annual maximum still water level versus annual maximum Potential Maximum Storm Tide (PMST); (b) cumulative distribution function based on observed annual maxima and PMST estimates; (c–h) the relationships of MSL with PMST, non-tidal residuals and diurnal/semidiurnal tidal constituents and over tides at Wyndham, Australia (Lat: −15.4533, Lon: 128.1017), a macro-tidal system with a mixed (mainly Semi-Diurnal) tidal regime. Red lines represent the linear regression line between variables in each panel.

Gale" of October 1869 (Wood, 1978). As it happened, an especially close conjunction of perigee and syzygy occurred on 5 October 1869, and was accompanied by a hurricane. The two together caused major devastation throughout the Canadian Maritime Provinces. Moreover, the major constituents do not have to be exactly in phase —maximum water levels are high for several days around a spring tides. In this regard, Wood (1978) defines a perigean spring tide as one in which perigee (closest approach of the earth and moon) and syzygy (alingment of the sun and moon) coincide within 36 hr; that is, within a 72 hr window. A pseudo-perigean spring tide, which can also cause very high waters, occurs with when perigee and syzygee coincide within 84 hr, providing a 7-day window. Diurnal tidal regimes have different periodicities, but the same principles applies. In summary, PMST is a conservative upper limit or threshold, useful for estimating the potentially highest storm tide based on the available record and as input for the design of critical infrastructure. To further demonstrate the applicability of PMST in design practices and its conservativeness we have provided a time-series of PMST annual max and the associated cumulative distribution function (CDF) in panels a and b of Figures 2–5, respectively. The CDF curves are drawn based on maximum likelihood estimates of the parameters of the generalized extreme value distributions at each gauge, and the still water level plus the associated annual maxima for PMST at the gauge. From these CDF curves, the design flood magnitude of a return period of interest can be obtained, that is, the CDF = 0.90 is associated with the height of a 10 year flood (annual exceedance probability of 0.1).

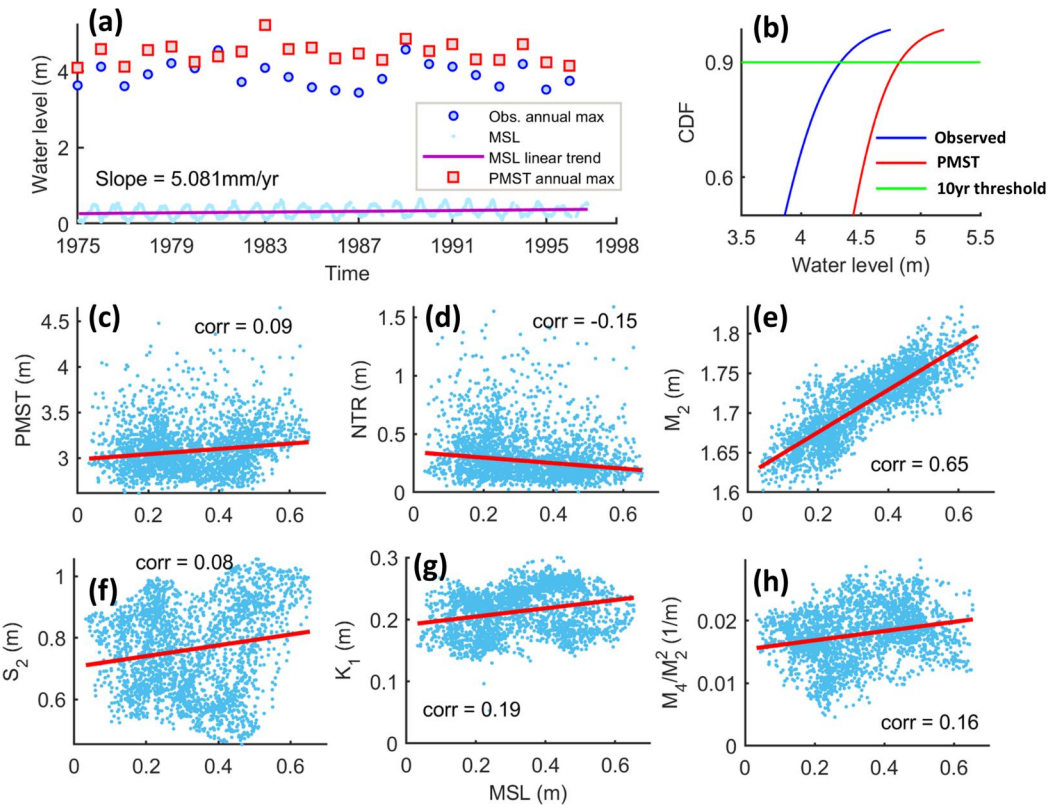

Figure 3. Trends and relationships at Lvsi, China. (a) Historic trends in mean sea level (MSL) and observed annual maximum still water level versus annual maximum Potential Maximum Storm Tide (PMST); (b) cumulative distribution function based on observed annual maxima and PMST estimates; (c–h) the relationships of MSL with PMST, non-tidal residuals and diurnal/semidiurnal tidal constituents and over tides at Lvsi, Jiangsu, China (Lat: 32.1333, Lon: 121.6167), a macro-tidal system with a semi-diurnal tidal regime. Red lines represent the linear regression line between variables in each panel.

We implement regression analysis to analyze how HTs and NTR have varied with MSL over the length of observation. For this purpose, we employ a robust linear regression scheme with reweighted least squares and a bisquare weighting function (Street et al., 1988). Such a robust method helps ensure the detected trend is not as sensitive to outliers, as it is in ordinary least square methods (Yu & Yao, 2017). The regression analysis implemented for each tidal component and NTR with MSL, one at a time. We assume that the estimated slope out of this robust regression analysis remains valid within the range of projected MSL in the following decades. Here, we also calculate Kendall rank correlation coefficient (CC) as a measure of dependence between variables (Kendall & Gibbons, 1990) and assume a significant correlation between variables if the p-value is <0.05.

We use MSL projections from Kopp et al. (2017) that integrate a probabilistic framework with a process model to estimate the likelihood of relative MSL rise above a reference (i.e., MSL in year 2000) at each location. These estimates are based on the framework proposed by Kopp et al. (2014) that uses a joint probability distribution for global mean thermal expansion and regional ocean dynamics. The regional contributions of nonclimatic factors are based upon a spatiotemporal statistical model of tide-gauge observations (Kopp et al., 2017). Here, we use the *near-term* projections, that is, for year 2050, under representative concentration pathway (RCP) 8.5, at which time the different RCPs (e.g., 2.6, 4.5, and 8.5) have not greatly deviated from one another (W. V. Sweet et al., 2022; van Vuuren et al., 2011). Realistic projection of ECWL and flooding beyond 2050 requires a comprehensive understanding of anthropogenic activities and protective measures to be implemented in the following decades. Also, MSL is not the only non-astronomical factor that modulate tides, and for a more comprehensive analysis of trends in coastal flooding beyond the mid-21st century, other factors contributing to ECWL like tectonic activity, shoreline position, hydrologic regime, and harbor modification should be taken into account (Haigh et al., 2019; Talke & Jay, 2020; Woodworth et al., 2019).

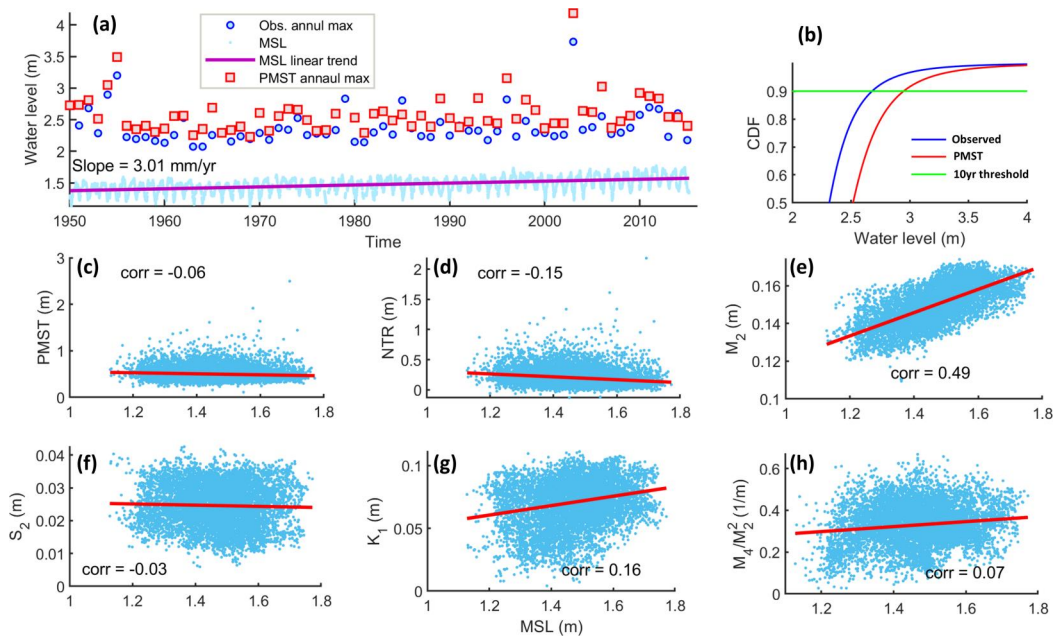

Figure 4. Trends and relationships at Baltimore, MD. (a) Historic trends in mean sea level (MSL) and observed annual maximum still water level versus annual maximum Potential Maximum Storm Tide (PMST); (b) cumulative distribution function based on observed annual maxima and PMST estimates; (c–h) the relationships of MSL with PMST, non-tidal residuals and diurnal/semidiurnal tidal constituents and over tides at Baltimore, MD, USA (Lat: 39.2667, Lon: −76.5783). Red lines represent the linear regression line between variables in each panel.

3. Results

3.1. Changes in the Storm Tide Regime Due To SLR

Relative MSL has risen in most (79%) locations studied here. The median rate of SLR among the gauges with a positive trend is 2.5 mm/yr (90% range of variability [i.e., 5th and 95th percentiles] of {0.4, 7.5 mm/yr}). The East and Gulf coasts of United States, southwestern coasts of Europe, East Asia and northern coasts of Australia generally show strong positive SLR rates. In contrast, gauges on the coasts of Alaska, Canada and in northern Europe, including Scandinavian Peninsula, generally show negative MSL change trends over the last few decades (Figure 1a). The positive SLR trend for majority of gauges across tropical Pacific Ocean found here is consistent with previous studies and particularly important as altered ECWL due to SLR and its associated flooding pose serious threat to the inhabitants of these areas (Church et al., 2006).

The locations that show significant SLR and a strongly positive relationship between PMST and MSL variations exhibit a variety of tidal/nontidal patterns. Metrics like tide-to-NTR ratio (Figure 1c) and overtide generation (Figure 1d) can help characterize these patterns and understand the underlying mechanisms deriving higher likelihood for ECWL. For example, at Wyndham (Northern Australia) there is a significant positive correlation between MSL and PMST; the CC is 0.28; with a 95% confidence bound of {0.27, 0.33}, caused mainly by the positive correlation between MSL and the solar semidiurnal tide S_2 (CC = 0.20; {0.18, 0.22}) and to a lesser extent by MSL and NTR (CC = 0.10; {0.08, 0.13}). Other components show a relatively weak relationship with MSL (Figure 2). Thus, at Wyndham a combination of rapid SLR (6.87 mm/yr), large tides with increasing S_2 amplitude, and intensified surge dynamics may increase flood hazard in the future. Given the strong interactions between various ECWL components in this location (and similar locations marked by red circles in both Figures 1a and 1b), flood hazard projections that ignore altered storm tide regime at a higher MSL are subject to a significant error (Boumis et al., 2023a). There are also, however, locations with positive relative SLR trends at which there is a negative relationship between MSL and other components of ECWL (i.e., East coast of United States and East Asia). In such cases, the approach based on linear combinations of current storm tide regime and the projected SLR yields an overly conservative estimates of flood hazard.

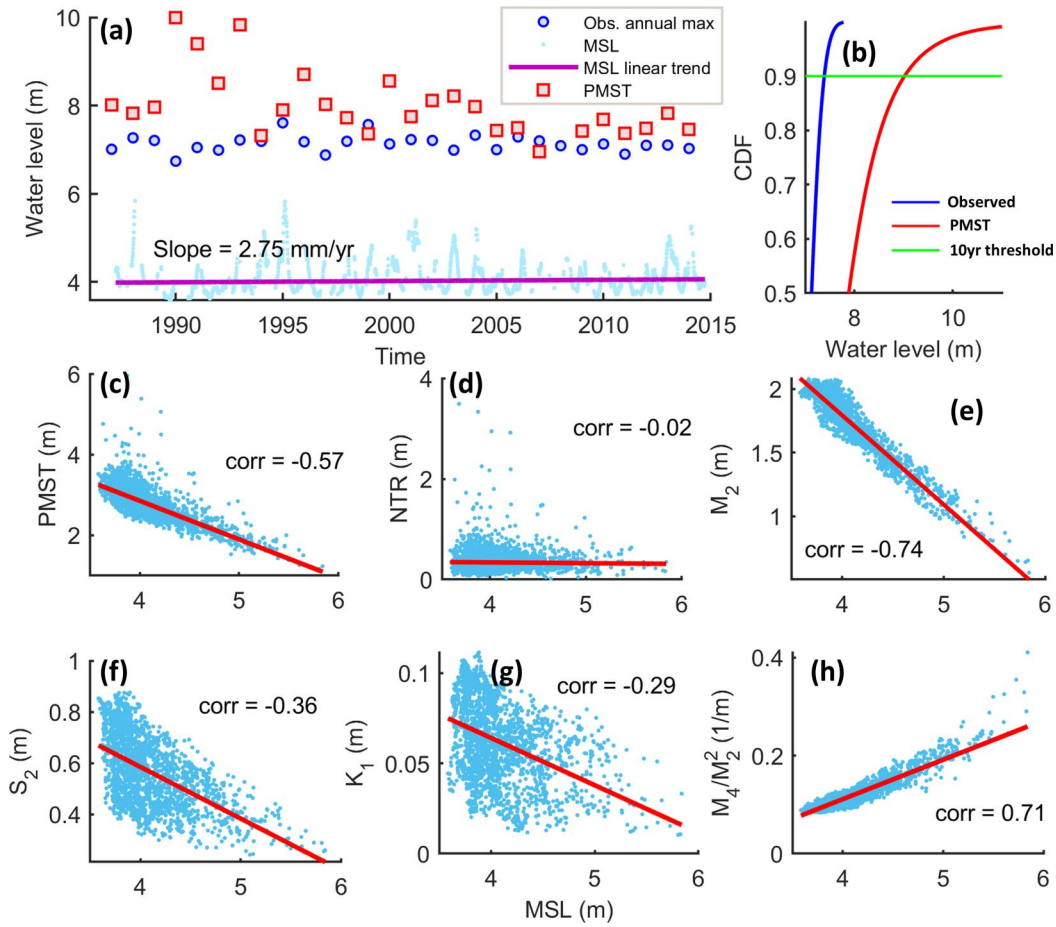

Figure 5. Trends and relationships at Nantes, France. (a) Historic trends in mean sea level (MSL) and observed annual maximum still water level versus annual maximum Potential Maximum Storm Tide (PMST); (b) cumulative distribution function based on observed annual maxima and PMST estimates; (c–h) the relationships of MSL with PMST, non-tidal residuals and diurnal/semidiurnal tidal constituents and overtides at Nantes Usine Bluree, France (Lat: 47.1935, Lon: −1.6337), a macro-tidal system with a semi-diurnal tidal regime. Red lines represent the linear regression line between variables in each panel.

The extent to which altered tidal amplitude at higher MSLs influences flooding dynamics depends on the tide-to-NTR ratio (Figure 1c). In Lvsi, Jiangsu (China) a relatively large HT to NTR ratio makes the lunar semidiurnal tide M_2 the dominant component that governs the relationship between PMST and MSL (Figure 3). In this case, despite a negative correlation (CC = −0.15; {−0.18, −0.13}) between NTR and MSL, a strong positive correlation between M_2 and MSL (CC = 0.65; {0.63–0.66}) and to a lesser extent K_1 and MSL (CC = 0.19; {0.17, 0.22}) produces a positive correlation between PMST and MSL (CC = 0.14; {0.11, 0.16}).

There are locations at which a relatively small HT to NTR ratio (i.e., <1) means that the relationship between MSL and NTR dominates the PMST regime. Baltimore, MD (USA) is an example. Despite a positive relationship between MSL and major HTs (e.g., K_1 and M_2), a negative correlation between MSL and NTR (CC = −0.15; {−0.17, −0.13}) controls the PMST regime; suggesting an insignificant contribution of nonlinearities in coastal flooding at higher MSLs (Figure 4). In cases like Baltimore with relatively small HT to NTR ratio (marked by bluish circles in Figure 1c), adding SLR projections to the estimated storm tide regime is adequate for planning purposes at present, though the storm tide regime may change in the future (Gori et al., 2022).

3.2. River Influence

Freshwater-influenced systems (e.g., estuaries, bays and deltas) behave differently from open coasts. Along a typical open coast, MSL rise implies deeper water, less friction and smaller overtides. As MSL increases, HT and

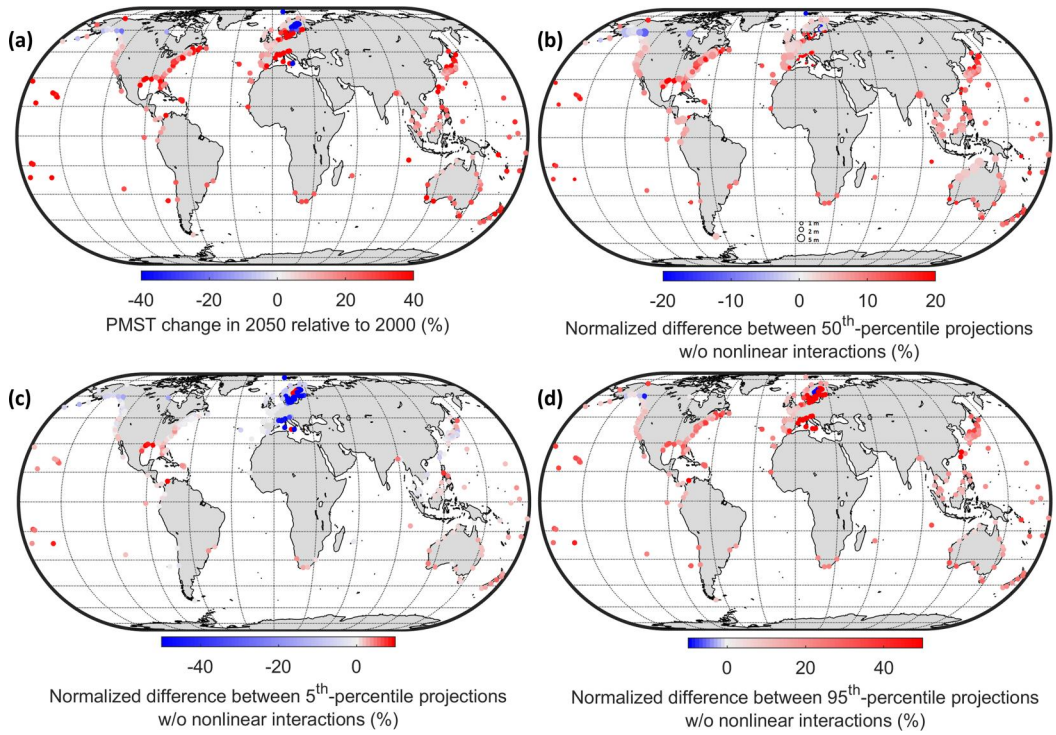

Figure 6. Projected changes in the drivers of future coastal flooding. (a) Estimated change in coastal extreme water level under projected Sea-level rise (SLR) by 2050 (SLR from Ref (Kopp et al., 2017)). (b–d) Normalized difference between the scenarios with and without considering nonlinear interactions between still water level components under 50th, 5th, and 95th percentile of SLR projection in year 2050, respectively. Size of the circles in panel b shows the estimated extreme water level in the future above mean sea level in year 2000.

NTR will (barring a major change in resonance) increase along with MSL, the increased greater diurnal tidal range needs to be considered in coastal flooding projections (Arns et al., 2017; Devlin, Jay, Talke, et al., 2017). Furuögrund (Sweden) is an example, at which tidal and non-tidal components are positively correlated with MSL variations. Nantes on the Loire Estuary (France), on the other hand, provides an example of the system where the interactions of river discharge and coastal water level tend to ameliorate flood hazard. Here, as in other similar systems (marked by red circles in Figure 1d), overtide ratio $M_4/M_2{}^2$ is positively correlated with MSL (Figure 5). Fort Pulaski, GA (USA) is another example where an analysis of the underlying dynamics and their compounding effects is necessary to understand how freshwater influx characteristics might change the ECWL regime under SLR (Muñoz et al., 2020, 2021). San Francisco Bay, CA is a location with relatively large HT to NTR ratio (reddish circles in Figure 1c) where overtides are positively correlated with MSL (reddish circles in Figure 1d), at which modeling the interactions between freshwater influx and coastal ocean water level is critical for accurate estimation of future coastal flooding. In such systems, understanding of oceanic processes is not sufficient for accurate estimation of SLR impacts on coastal flooding, and a coupled hydrologic-hydrodynamics modeling framework is vital for accurate estimation of flood risk (Bakhtyar et al., 2020; Bilskie et al., 2021; Moftakhari et al., 2019; Santiago-Collazo et al., 2019; Ye et al., 2020).

3.3. Extreme Water Level Dynamics Changes With SLR

The median projected relative SLR by mid-century (under RCP 8.5) suggests that global median PMST will increase 20% relative to year 2000 (Figure 6a; 90% range of variability {−30%, +84%}). This increase is regionally variable and more pronounced (24% larger; 90% range of variability of {9%, 59%}) in the tropics (latitude −30° to +30°). To quantify the contribution of nonlinear interactions in altered ECWL regime, we calculate the normalized difference between projected PMST with and without adjustments for the nonlinear interactions shown in Figures 6b–6d. The median difference under 50th percentile SLR scenario across all studied gauges is 10% with a strong regional variability (90% range of variability {−6%, +41%}). This range of

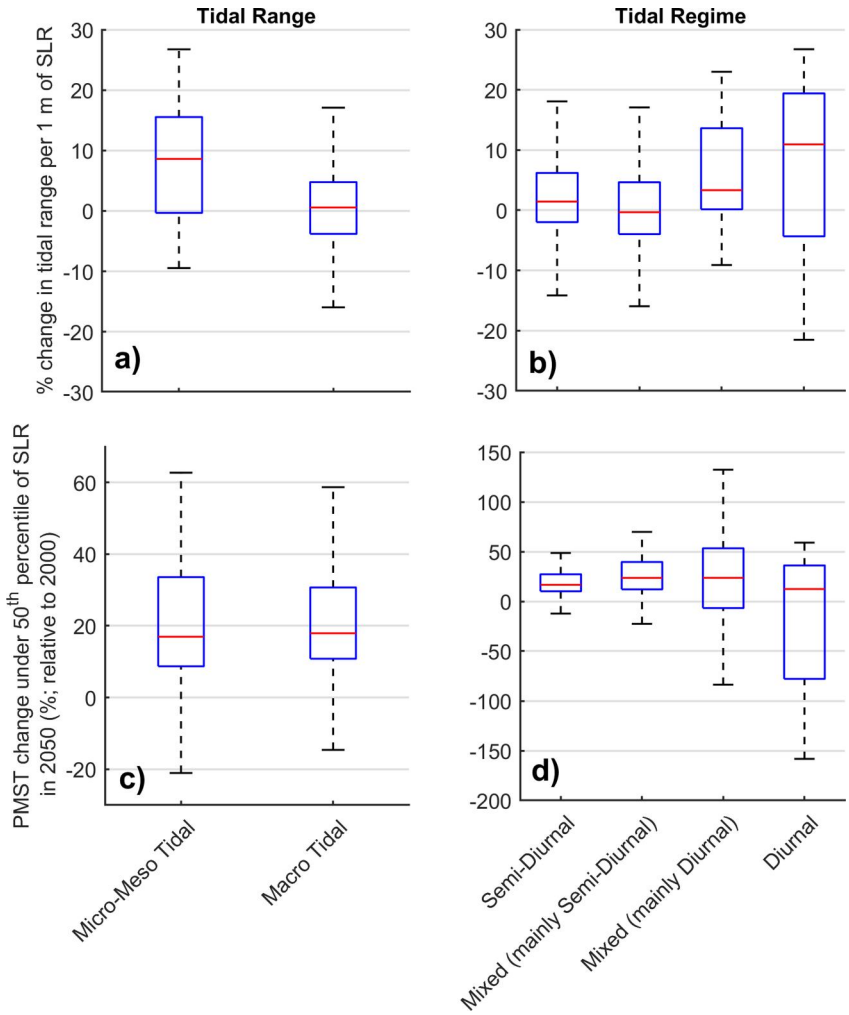

Figure 7. Response of different tidal systems to Sea-level rise (SLR). Estimated historic (panels a and b) and projected (panels c and d) change in coastal extreme water level. Future estimates are under 50th percentile of projected SLR by 2050 (SLR under representative concentration pathway 8.5 from Kopp et al. (2017)).

variability is much wider in temperate and higher latitudes (latitude >45°), where one-fourth of gauges are located and median normalized difference under 50th percentile SLR scenario is 3.5% (90% range of variability {−84%, +59%}). Thus, ignoring nonlinear interactions between tidal and non-tidal components of ECWL under SLR may yield significant error in estimated flooding hazards by mid-century, but results vary regionally and locally.

The contribution of nonlinear interactions becomes even more important under extreme SLR scenarios (e.g., 5th and 95th percentiles). The median of aforementioned normalized difference under the 95th percentile of SLR scenario increases to 20%, with strong regional patterns (90% range of variability {5%, 286%}), and a wider range of variability in latitudes >45° with 15% normalized difference and 90% range of variability {−6%, 448%}. These results indicate that: (a) including nonlinear interactions generally yields a higher estimated PMST increase; and (b) the increase may be up to a factor of four relative to a conventional approach, where the current storm tide regime is moved up at the rate of projected SLR.

3.4. Effects of Tidal Range and Regime on Variability

Tidal statistics can help characterize the potential response of ECWL to SLR. These systems can be classified into three categories based on their tidal amplitude, namely: micro-tidal (<0.5 m), meso-tidal (0.5–1.75 m), and macro-tidal (>1.75 m) (Passeri et al., 2015). Micro- and meso-tidal systems are more susceptible to SLR than macro-tidal systems (Figure 7). Based on the historic records, the median increase in tidal range in micro- and

meso-tidal systems has been 9% (with 25th and 75th percentiles of 0% and 15%, respectively); in contrast to macro-tidal systems at which no significant change is detected (Figure 7a).

Following the NOAA tidal glossary (NOAA-COOPS, 2000) we also use F, the amplitude ratio of $K_1 + O_1$ to $M_2 + S_2$, to classify tidal regime in studied systems. We detect a significant difference between systems with different tidal regimes. Systems with diurnal ($F > 3.0$) and mixed-mainly diurnal ($1.5 < F < 3.0$) regime are more sensitive to MSL change than systems with semidiurnal ($F < 0.25$) and mixed-mainly semidiurnal ($0.25 < F < 1.5$) tidal regime. Diurnal systems have been the most susceptible systems to SLR with median increased tidal range of 11% (with 25th and 75th percentiles to be −4 and 19%, respectively) over the past few decades (Figure 7b).

The tidal range and regime classification provides good insight towards expected change in PMST over the next few decades. The expected change in PMST under 50th percentile of projected SLR by 2050 in micro- and meso-tidal systems (median = 17%) does not seem to be significantly different from macro-tidal systems (median = 18%); however the range of variability is wider for systems with smaller tidal amplitude (Figure 7c), probably because a particular absolute change represents a higher percentage change in these systems. Also, while the median change in PMST under projected SLR by 2050 ranges between 12% and 24% in the four different tidal regimes, systems with diurnal regime show more variability compared with semidiurnal ones (Figure 7d).

4. Discussion

4.1. Utility of PMST

For planning purposes, it is vital to know how a harbor or region will respond to the next Saxby tide or Hurricane Sandy. Accordingly, PMST provides an estimate of an upper limit threshold on inundation in coming decades, useful for estimating the potentially highest storm tide associated with a given forcing or event. It can, therefore, inform design of critical infrastructure, without needing or intending to be the only necessary measure.

Numerical modeling is an alternative or complementary approach to data-driven analyses, like the one proposed here. Indeed, use of numerical models is a critical aspect of many coastal scientific/engineering endeavors. However, validation of coastal modeling, especially in areas with complex bathymetry/topography and dynamics, presents inherent challenges. In some places, despite advancements in technology such as Lidar, obtaining precise topographical data remains challenging, even when benchmarks are available for reference. Bathymetric data are often insufficient in quality and quantity to provide model results of the quality needed for practical needs. We emphasize that use of a data-driven method is not intended to replace traditional modeling approaches, but rather to supplement them. PMST methodology provides a valuable and cost-effective alternative, particularly for obtaining a preliminary understanding of the coastal dynamics. While it does not replace detailed studies necessary for constructing facilities, it serves as an efficient and economical means for an initial assessment. Thus, the choice between modeling approaches is not binary; rather, it is contingent on the specific objectives and circumstances. A data-driven methods like ours, by virtue of its cost-effectiveness, is well-suited for providing an initial overview, allowing researchers and stakeholders to identify areas that necessitate more detailed investigation. This approach is particularly advantageous in scenarios where resource constraints or time limitations may impede the feasibility of extensive modeling endeavors.

4.2. Possible Limitations

Some of the general conclusions drawn here may be affected by regional biases in the GESLA-2 data base, which has incomplete coverage along the African coasts and South America and southwest Asia, as compared to nearly full coverage of North America, Europe and East Asia. This regional bias yields, for example, no or fewer samples from diurnal macro tidal stations (e.g., Sea of Okhotsk). Another factor contributing to regional bias is the insufficient number of inland tide gauges installed in estuarine systems, in contrast to coastal areas. This lack of comprehensive coverage could result in uncertainties regarding our comprehension of freshwater-influenced tidal systems and their response to SLR (Khojasteh et al., 2023). A fuller range of stations would provide additional understanding of HT-NTR-MSL interactions and might change some of our interpretations of broad patterns. However, better data coverage would not change the interpretation of results at stations analyzed, or future use of the tool for practical purposes.

The timeseries length threshold used here was 19 yr. This is sufficient for various tidal analysis purposes, but records lengths less than about 50 yr that are not integral lengths of tidal periodicities such as 4.4, 8.8, and 18.6 yrs can yield biases in constituent trends. To minimize this problem, we have used the nodal variation feature of *t_tide*. Moreover, use of the 19-yr threshold, ensures inclusion of a large number of stations. Thus, while some bias associated with record length may affect results at individual stations, especially at those with larger influence of storm surge in PMST dynamics, these are likely to be averaged out regionally. Moreover, use of a longer timeseries and/or advanced statistical methods that enable sharing information across gauged locations (Boumis et al., 2023b; Rashid et al., 2024) would help with the problems regarding the regional biases mentioned above.

There is a potential uncertainty in using nodal correction feature of *t_tide*. Many stations, especially those in shallower coasts, do not follow the theoretical nodal cycle pattern used by *t_tide* (Feng et al., 2015; Woodworth, 2010). There are studies that have found estimates based on standard nodal corrections close enough to those based on empirical corrections (Ray & Foster, 2016; Ray & Talke, 2019). Thus, here we assume that this potential source of uncertainty does not significantly influence the global patterns recognized and so the conclusions remain valid.

With a focus on tidal constituents and their variability with SLR at Global scale, our analysis does not take important local processes, that is, rainfall/runoff regime, baroclinic effects, wave setup, steric effects and other anthropogenic effects (i.e., dredging) that significantly affect the tidal regime, especially in estuarine systems (Dykstra et al., 2022; Familkhalili et al., 2020; Khojasteh et al., 2021, 2022; Passeri et al., 2016) and in southeast Asia (Devlin et al., 2018). Thus, while our results are helpful for understanding the behavior of tides in the face of SLR, accurate prediction of extreme sea level at local scale requires consideration of local processes and engineering alterations.

Seasonal patterns are important in ECWL estimation in many locations. They have not been considered in our long-term Global analysis, in part because these patterns are variable between stations. In fact, seasonality in tidal and non-tidal components and even in their dependence structure can pose a significant uncertainty in ECWL estimates (D'Arcy et al., 2021; Devlin et al., 2018; Nasr et al., 2021). This could be dealt with in future studies in several ways, for example, use of a probabilistic approach that allows inclusion of seasonal effects, or use of seasonal regression models. Because seasonal patterns vary widely between stations and regions, such an approach was not practical here and better carried out at a local or regional scale.

Here, the determination of the PMST does not rely on establishing an upper limit for the NTR at each step of the calculation. Achieving such an upper limit necessitates an exhaustive hydrometeorological analysis, coupled with detailed ocean circulation models, and the generation of a large number of ensembles that reasonably represent potential scenarios (H. Li et al., 2023). Instead, PMST is derived based on the actual magnitude that this stochastic variable has taken at any given step. The surge activity is also assumed to be changing only with SLR. In fact the surge dynamics are subject to future change in a warming climate as its atmospheric drivers vary (Gori et al., 2022; Grinsted et al., 2013; Marsooli et al., 2019). Our analysis method, however, captures both changes in NTR directly related to MSL rise, and those that are driven by atmospheric proceses that are correlated with, but not caused by, MSL rise. Moreover, PMST is deliberately conservative, and we do not extend the analysis beyond 2050, because of the likelihood that NTR and MSL dynamics will change in ways that cannot be predicted with our methods. Thus, lack of a model for how NTR will change in the future is a conceptual limitation, but up to 2050, probably not a practical one.

Finally, the correlations between the various components of the water level spectrum that the PMST procedure reveals are also practically important in themselves, not just for their contribution to the PMST statistic. If an engineer knows that, for example, tides and/or surge increase at a particular location as MSL rises, this suggests both more detailed investigations, and a conservative design approach. This would be especially true in situations where the water level record is short and storm surges large. Thus, the PMST calculation may have value even when the sea level record is undesirably short.

5. Conclusions

Overall, we detect a significant correlation between MSL variability and PMST at 89% of locations studied around the globe. In 42% of these locations (37% of the total studied gauges) MSL is rising over time, and there is

a significant positive correlation between MSL variation and PMST. Thus, ignoring nonlinear interactions between SLR and storm tide may cause underestimation of coastal flooding risk in the future at almost one-third of studied locations (e.g., in western Pacific, northern Atlantic, and northern coasts of Australia).

In 72% of the studied locations, we expect a higher ECWL by the mid-century (where PMST shows positive trends), though the rates and pattern of these increased flood hazards are different between various systems. Among all studied sites, the 27% of systems with micro- and meso-tidal range and with diurnal tidal regime are most sensitive to SLR. This means there is no single recipe for SLR adaptation around the world. Depending on the local MSL trend, the tidal range and regime (diurnal vs. semidiurnal) of the system of interest, and the strength of interactions between various ECWL components (MSL, HT, and NTR), different preventive measures should be implemented to ensure resilience in the face of increasing flood hazards.

Conflict of Interest

The authors declare no conflicts of interest relevant to this study.

Data Availability Statement

The water level data for tide gauges around the globe are obtained from the GESLA-2 database (https://gesla787883612.wordpress.com/gesla2/).

Acknowledgments
The authors thank the editor and three anonymous reviewers for their constructive comments. This study is funded by NSF award 2223893. Also, Hamed Moftakhari was partially supported by NSF award 2238000.

References

Arns, A., Dangendorf, S., Jensen, J., Talke, S., Bender, J., & Pattiaratchi, C. (2017). Sea-level rise induced amplification of coastal protection design heights. *Scientific Reports*, *7*(1), 40171. https://doi.org/10.1038/srep40171

Arns, A., Wahl, T., Wolff, C., Vafeidis, A. T., Haigh, I. D., Woodworth, P. L., et al. (2020). Non-linear interaction modulates global extreme sea levels, coastal flood exposure, and impacts. *Nature Communications*, *11*(1), 1918. https://doi.org/10.1038/s41467-020-15752-5

Bakhtyar, R., Maitaria, K., Velissariou, P., Trimble, B., Mashriqui, H., Moghimi, S., et al. (2020). A new 1D/2D coupled modeling approach for a riverine-estuarine system under storm events: Application to Delaware river basin. *Journal of Geophysical Research: Oceans*, *125*(9), e2019JC015822. https://doi.org/10.1029/2019JC015822

Bilskie, M. V., Angel, D., Yoskowitz, D., & Hagen, S. C. (2022). Future flood risk exacerbated by the dynamic impacts of sea level rise along the northern Gulf of Mexico. *Earth's Future*, *10*(4), e2021EF002414. https://doi.org/10.1029/2021EF002414

Bilskie, M. V., Hagen, S. C., Alizad, K., Medeiros, S. C., Passeri, D. L., Needham, H. F., & Cox, A. (2016). Dynamic simulation and numerical analysis of hurricane storm surge under sea level rise with geomorphologic changes along the northern Gulf of Mexico. *Earth's Future*, *4*(5), 177–193. https://doi.org/10.1002/2015EF000347

Bilskie, M. V., Zhao, H., Resio, D., Atkinson, J., Cobell, Z., & Hagen, S. C. (2021). Enhancing flood hazard assessments in coastal Louisiana through coupled hydrologic and surge processes. *Frontiers in Water*, *3*, 609231. https://doi.org/10.3389/frwa.2021.609231

Boumis, G., Moftakhari, H. R., & Moradkhani, H. (2023a). Coevolution of extreme sea levels and sea-level rise under global warming. *Earth's Future*, *11*(7), e2023EF003649. https://doi.org/10.1029/2023EF003649

Boumis, G., Moftakhari, H. R., & Moradkhani, H. (2023b). Storm surge hazard estimation along the US Gulf coast: A bayesian hierarchical approach. *Coastal Engineering*, *185*, 104371. https://doi.org/10.1016/j.coastaleng.2023.104371

Bromirski, P. D., & Cayan, D. R. (2015). Wave power variability and trends across the North Atlantic influenced by decadal climate patterns. *Journal of Geophysical Research: Oceans*, *120*(5), 3419–3443. https://doi.org/10.1002/2014JC010440

Buchanan, M. K., Kopp, R. E., Oppenheimer, M., & Tebaldi, C. (2016). Allowances for evolving coastal flood risk under uncertain local sea-level rise. *Climatic Change*, *137*(3–4), 347–362. https://doi.org/10.1007/s10584-016-1664-7

Calafat, F. M., Wahl, T., Tadesse, M. G., & Sparrow, S. N. (2022). Trends in Europe storm surge extremes match the rate of sea-level rise. *Nature*, *603*(7903), 841–845. https://doi.org/10.1038/s41586-022-04426-5

Cheung, K. F., Wei, Y., Yamazaki, Y., & Yim, S. C. S. (2011). Modeling of 500-year tsunamis for probabilistic design of coastal infrastructure in the Pacific Northwest. *Coastal Engineering*, *58*(10), 970–985. https://doi.org/10.1016/j.coastaleng.2011.05.003

Church, J. A., White, N. J., & Hunter, J. R. (2006). Sea-level rise at tropical Pacific and Indian Ocean islands. *Global and Planetary Change*, *53*(3), 155–168. https://doi.org/10.1016/j.gloplacha.2006.04.001

Dangendorf, S., Hay, C., Calafat, F. M., Marcos, M., Piecuch, C. G., Berk, K., & Jensen, J. (2019). Persistent acceleration in global sea-level rise since the 1960s. *Nature Climate Change*, *9*(9), 705–710. https://doi.org/10.1038/s41558-019-0531-8

D'Arcy, E., Tawn, J., Joly-Lagugel, A., & Sifnioti, D. (2021). Accounting for seasonality in extreme sea level estimation (other). *pico*. https://doi.org/10.5194/egusphere-egu21-12276

De Dominicis, M., Wolf, J., Jevrejeva, S., Zheng, P., & Hu, Z. (2020). Future interactions between sea level rise, tides, and storm surges in the world's largest urban area. *Geophysical Research Letters*, *47*(4), e2020GL087002. https://doi.org/10.1029/2020GL087002

Devlin, A. T., Jay, D. A., Talke, S. A., & Zaron, E. (2014). Can tidal perturbations associated with sea level variations in the western Pacific Ocean be used to understand future effects of tidal evolution? *Ocean Dynamics*, *64*(8), 1093–1120. https://doi.org/10.1007/s10236-014-0741-6

Devlin, A. T., Jay, D. A., Talke, S. A., Zaron, E. D., Pan, J., & Lin, H. (2017). Coupling of sea level and tidal range changes, with implications for future water levels. *Scientific Reports*, *7*(1), 17021. https://doi.org/10.1038/s41598-017-17056-z

Devlin, A. T., Jay, D. A., Zaron, E. D., Talke, S. A., Pan, J., & Lin, H. (2017). Tidal variability related to sea level variability in the Pacific Ocean. *Journal of Geophysical Research: Oceans*, *122*(11), 8445–8463. https://doi.org/10.1002/2017JC013165

Devlin, A. T., Pan, J., & Lin, H. (2019). Extended spectral analysis of tidal variability in the North Atlantic ocean. *Journal of Geophysical Research: Oceans*, *124*(1), 506–526. https://doi.org/10.1029/2018JC014694

Devlin, A. T., Zaron, E. D., Jay, D. A., Talke, S. A., & Pan, J. (2018). Seasonality of tides in southeast Asian waters. *Journal of Physical Oceanography*, *48*(5), 1169–1190. https://doi.org/10.1175/JPO-D-17-0119.1

Dykstra, S. L., & Dzwonkowski, B. (2021). The role of intensifying precipitation on coastal river flooding and compound river-storm surge events, Northeast Gulf of Mexico. *Water Resources Research*, *57*(11), e2020WR029363. https://doi.org/10.1029/2020WR029363

Dykstra, S. L., Dzwonkowski, B., & Torres, R. (2022). The role of river discharge and geometric structure on diurnal tidal dynamics, Alabama, USA. *Journal of Geophysical Research: Oceans*, *127*(3), e2021JC018007. https://doi.org/10.1029/2021JC018007

Faber, M. H., & Stewart, M. G. (2003). Risk assessment for civil engineering facilities: Critical overview and discussion. *Reliability Engineering & System Safety*, *80*(2), 173–184. https://doi.org/10.1016/S0951-8320(03)00027-9

Familkhalili, R., & Talke, S. A. (2016). The effect of channel deepening on tides and storm surge: A case study of Wilmington, NC: The alteration of tides and storm surge. *Geophysical Research Letters*, *43*(17), 9138–9147. https://doi.org/10.1002/2016GL069494

Familkhalili, R., Talke, S. A., & Jay, D. A. (2020). Tide-storm surge interactions in highly altered estuaries: How channel deepening increases surge vulnerability. *Journal of Geophysical Research: Oceans*, *125*(4), e2019JC015286. https://doi.org/10.1029/2019JC015286

Feng, X., Tsimplis, M. N., & Woodworth, P. L. (2015). Nodal variations and long-term changes in the main tides on the coasts of China. *Journal of Geophysical Research: Oceans*, *120*(2), 1215–1232. https://doi.org/10.1002/2014JC010312

Fernández-Montblanc, T., Vousdoukas, M. I., Ciavola, P., Voukouvalas, E., Mentaschi, L., Breyiannis, G., et al. (2019). Towards robust pan-European storm surge forecasting. *Ocean Modelling*, *133*, 129–144. https://doi.org/10.1016/j.ocemod.2018.12.001

Goodwin, P., Haigh, I. D., Rohling, E. J., & Slangen, A. (2017). A new approach to projecting 21st century sea-level changes and extremes. *Earth's Future*, *5*(2), 240–253. https://doi.org/10.1002/2016EF000508

Gori, A., Lin, N., Xi, D., & Emanuel, K. (2022). Tropical cyclone climatology change greatly exacerbates US extreme rainfall–surge hazard. *Nature Climate Change*, *12*(2), 171–178. https://doi.org/10.1038/s41558-021-01272-7

Gregory, J. M., Griffies, S. M., Hughes, C. W., Lowe, J. A., Church, J. A., Fukimori, I., et al. (2019). Concepts and terminology for sea level: Mean, variability and change, both local and global. *Surveys in Geophysics*, *40*(6), 1251–1289. https://doi.org/10.1007/s10712-019-09525-z

Grinsted, A., Moore, J. C., & Jevrejeva, S. (2013). Projected Atlantic hurricane surge threat from rising temperatures. *Proceedings of the National Academy of Sciences*, *110*(14), 5369–5373. https://doi.org/10.1073/pnas.1209980110

Guo, L., van der Wegen, M., Jay, D. A., Matte, P., Wang, Z. B., Roelvink, D., & He, Q. (2015). River-tide dynamics: Exploration of nonstationary and nonlinear tidal behavior in the Yangtze River estuary. *Journal of Geophysical Research: Oceans*, *120*(5), 3499–3521. https://doi.org/10.1002/2014JC010491

Haigh, I. D., Pickering, M. D., Green, J. A. M., Arbic, B. K., Arns, A., Dangendorf, S., et al. (2019). The tides they are a-Changin': A comprehensive review of past and future non-astronomical changes in tides, their driving mechanisms and future implications. *Reviews of Geophysics*, *58*(1), e2018RG000636. https://doi.org/10.1029/2018RG000636

Hinkel, J., Lincke, D., Vafeidis, A. T., Perrette, M., Nicholls, R. J., Tol, R. S. J., et al. (2014). Coastal flood damage and adaptation costs under 21st century sea-level rise. *Proceedings of the National Academy of Sciences*, *111*(9), 3292–3297. https://doi.org/10.1073/pnas.1222469111

Hoitink, A. J. F., & Jay, D. A. (2016). Tidal river dynamics: Implications for deltas. *Reviews of Geophysics*, *54*(1), 240–272. https://doi.org/10.1002/2015RG000507

Hunter, J. (2012). A simple technique for estimating an allowance for uncertain sea-level rise. *Climatic Change*, *113*(2), 239–252. https://doi.org/10.1007/s10584-011-0332-1

Idier, D., Dumas, F., & Muller, H. (2012). Tide-surge interaction in the English channel. *Natural Hazards and Earth System Sciences*, *12*(12), 3709–3718. https://doi.org/10.5194/nhess-12-3709-2012

Idier, D., Paris, F., Cozannet, G. L., Boulahya, F., & Dumas, F. (2017). Sea-level rise impacts on the tides of the European Shelf. *Continental Shelf Research*, *137*, 56–71. https://doi.org/10.1016/j.csr.2017.01.007

IPCC. (2019). IPCC special report on the ocean and cryosphere in a changing climate. Retrieved from https://www.ipcc.ch/srocc/

Jay, D. A. (2009). Evolution of tidal amplitudes in the eastern Pacific Ocean. *Geophysical Research Letters*, *36*(4), L04603. https://doi.org/10.1029/2008GL036185

Jay, D. A., Devlin, A. T., Idier, D., Prokocki, E. W., & Flick, R. E. (2021). Tides and coastal geomorphology: The role of non-stationary processes. In *Reference module in earth systems and environmental sciences*. Elsevier. https://doi.org/10.1016/B978-0-12-818234-5.00166-8

Jay, D. A., Leffler, K., Diefenderfer, H. L., & Borde, A. B. (2015). Tidal-Fluvial and estuarine processes in the lower Columbia river: I. Along-channel water level variations, Pacific Ocean to Bonneville Dam. *Estuaries and Coasts*, *38*(2), 415–433. https://doi.org/10.1007/s12237-014-9819-0

Johnson, G. C., & Lyman, J. M. (2020). Warming trends increasingly dominate global ocean. *Nature Climate Change*, *10*(8), 757–761. https://doi.org/10.1038/s41558-020-0822-0

Karamouz, M., Zoghi, A., & Mahmoudi, S. (2022). Flood modeling in coastal cities and flow through vegetated BMPs: Conceptual design. *Journal of Hydrologic Engineering*, *27*(10), 04022022. https://doi.org/10.1061/(ASCE)HE.1943-5584.0002206

Kendall, M. G., & Gibbons, J. D. (1990). *Rank correlation methods* (5th ed.). E. Arnold, Oxford University Press.

Khojasteh, D., Felder, S., Heimhuber, V., & Glamore, W. (2023). A global assessment of estuarine tidal response to sea level rise. *Science of the Total Environment*, *894*, 165011. https://doi.org/10.1016/j.scitotenv.2023.165011

Khojasteh, D., Glamore, W., Heimhuber, V., & Felder, S. (2021). Sea level rise impacts on estuarine dynamics: A review. *Science of the Total Environment*, *780*, 146470. https://doi.org/10.1016/j.scitotenv.2021.146470

Khojasteh, D., Ruprecht, J., Waddington, K., Moftakhari, H., AghaKouchak, A., & Glamore, W. (2022). Challenges of sea-level rise on estuarine tidal dynamics. In J. Humphreys & S. Little (Eds.), *Challenges in estuarine and coastal science* (pp. 45–58). Pelagic Publishing. https://doi.org/10.53061/VYYD7091

Kopp, R. E., DeConto, R. M., Bader, D. A., Hay, C. C., Horton, R. M., Kulp, S., et al. (2017). Evolving understanding of Antarctic ice-sheet physics and ambiguity in probabilistic sea-level projections. *Earth's Future*, *5*(12), 1217–1233. https://doi.org/10.1002/2017EF000663

Kopp, R. E., Horton, R. M., Little, C. M., Mitrovica, J. X., Oppenheimer, M., Rasmussen, D. J., et al. (2014). Probabilistic 21st and 22nd century sea-level projections at a global network of tide-gauge sites. *Earth's Future*, *2*(8), 383–406. https://doi.org/10.1002/2014EF000239

Kulp, S. A., & Strauss, B. H. (2019). New elevation data triple estimates of global vulnerability to sea-level rise and coastal flooding. *Nature Communications*, *10*(1), 4844. https://doi.org/10.1038/s41467-019-12808-z

Leffler, K. E., & Jay, D. A. (2009). Enhancing tidal harmonic analysis: Robust (hybrid) solutions. *Continental Shelf Research*, *29*(1), 78–88. https://doi.org/10.1016/j.csr.2008.04.011

Li, H., Haer, T., Couasnon, A., Enríquez, A. R., Muis, S., & Ward, P. J. (2023). A spatially-dependent synthetic global dataset of extreme sea level events. *Weather and Climate Extremes*, *41*, 100596. https://doi.org/10.1016/j.wace.2023.100596

Li, S., Wahl, T., Talke, S. A., Jay, D. A., Orton, P. M., Liang, X., et al. (2021). Evolving tides aggravate nuisance flooding along the U.S. coastline. *Science Advances*, *7*(10), eabe2412. https://doi.org/10.1126/sciadv.abe2412

Marcos, M., Calafat, F. M., Berihuete, Á., & Dangendorf, S. (2015). Long-term variations in global sea level extremes. *Journal of Geophysical Research: Oceans*, *120*(12), 8115–8134. https://doi.org/10.1002/2015JC011173

Marsooli, R., Lin, N., Emanuel, K., & Feng, K. (2019). Climate change exacerbates hurricane flood hazards along US Atlantic and Gulf Coasts in spatially varying patterns. *Nature Communications*, *10*(1), 3785. https://doi.org/10.1038/s41467-019-11755-z

Matte, P., Jay, D. A., & Zaron, E. D. (2013). Adaptation of classical tidal harmonic analysis to nonstationary tides, with application to river tides. *Journal of Atmospheric and Oceanic Technology*, *30*(3), 569–589. https://doi.org/10.1175/JTECH-D-12-00016.1

Mawdsley, R. J., & Haigh, I. D. (2016). Spatial and temporal variability and long-term trends in skew surges globally. *Frontiers in Marine Science*, *3*, 29. https://doi.org/10.3389/fmars.2016.00029

Melet, A., Meyssignac, B., Almar, R., & Le Cozannet, G. (2018). Under-estimated wave contribution to coastal sea-level rise. *Nature Climate Change*, *8*(3), 234–239. https://doi.org/10.1038/s41558-018-0088-y

Moftakhari, H., Schubert, J. E., AghaKouchak, A., Matthew, R. A., & Sanders, B. F. (2019). Linking statistical and hydrodynamic modeling for compound flood hazard assessment in tidal channels and estuaries. *Advances in Water Resources*, *128*, 28–38. https://doi.org/10.1016/j.advwatres.2019.04.009

Moftakhari, H. R., Jay, D. A., Talke, S. A., Kukulka, T., & Bromirski, P. D. (2013). A novel approach to flow estimation in tidal rivers. *Water Resources Research*, *49*(8), 4817–4832. https://doi.org/10.1002/wrcr.20363

Morim, J., Trenham, C., Hemer, M., Wang, X. L., Mori, N., Casas-Prat, M., et al. (2020). A global ensemble of ocean wave climate projections from CMIP5-driven models. *Scientific Data*, *7*(1), 105. https://doi.org/10.1038/s41597-020-0446-2

Muis, S., Apecechea, M. I., Dullaart, J., de Lima Rego, J., Madsen, K. S., Su, J., et al. (2020). A high-resolution global dataset of extreme sea levels, tides, and storm surges, including future projections. *Frontiers in Marine Science*, *7*, 263. https://doi.org/10.3389/fmars.2020.00263

Muis, S., Lin, N., Verlaan, M., Winsemius, H. C., Ward, P. J., & Aerts, J. C. J. H. (2019). Spatiotemporal patterns of extreme sea levels along the western North-Atlantic coasts. *Scientific Reports*, *9*(1), 3391. https://doi.org/10.1038/s41598-019-40157-w

Muis, S., Verlaan, M., Winsemius, H. C., Aerts, J. C. J. H., & Ward, P. J. (2016). A global reanalysis of storm surges and extreme sea levels. *Nature Communications*, *7*(1), 11969. https://doi.org/10.1038/ncomms11969

Muñoz, D. F., Moftakhari, H., & Moradkhani, H. (2020). Compound effects of flood drivers and wetland elevation correction on coastal flood hazard assessment. *Water Resources Research*, *56*(7), e2020WR027544. https://doi.org/10.1029/2020WR027544

Muñoz, D. F., Muñoz, P., Moftakhari, H., & Moradkhani, H. (2021). From local to regional compound flood mapping with deep learning and data fusion techniques. *Science of the Total Environment*, *782*, 146927. https://doi.org/10.1016/j.scitotenv.2021.146927

Nasr, A. A., Wahl, T., Rashid, M. M., Camus, P., & Haigh, I. D. (2021). Assessing the dependence structure between oceanographic, fluvial, and pluvial flooding drivers along the United States coastline. In *Coasts and estuaries/modelling approaches*. https://doi.org/10.5194/hess-2021-268

Neumann, B., Vafeidis, A. T., Zimmermann, J., & Nicholls, R. J. (2015). Future coastal population growth and exposure to Sea-Level rise and coastal flooding—A global assessment. *PLoS One*, *10*(3), e0118571. https://doi.org/10.1371/journal.pone.0118571

Nicholls, R. J., Hanson, S., Lowe, J. A., Slangen, A. B. A., Wahl, T., Hinkel, J., & Long, A. J. (2021). Integrating new sea-level scenarios into coastal risk and adaptation assessments: An ongoing process. *Wiley Interdisciplinary Reviews: Climate Change*, *12*(3), e706. https://doi.org/10.1002/wcc.706

NOAA-COOPS. (2000). *Tide and current glossary*. Silver Spring Maryland. Retrieved from https://www.tidesandcurrents.noaa.gov/publications/glossary2.pdf

Palmer, M. D., Gregory, J. M., Bagge, M., Calvert, D., Hagedoorn, J. M., Howard, T., et al. (2020). Exploring the drivers of global and local sea-level change over the 21st century and beyond. *Earth's Future*, *8*(9), e2019EF001413. https://doi.org/10.1029/2019EF001413

Parker, B. B. (2007). *Tidal analysis and prediction (No. NOAA special publication NOS CO-OPS 3)*. NOAA. Retrieved from https://tidesandcurrents.noaa.gov/publications/Tidal_Analysis_and_Predictions.pdf

Passeri, D. L., Hagen, S. C., Medeiros, S. C., Bilskie, M. V., Alizad, K., & Wang, D. (2015). The dynamic effects of sea level rise on low-gradient coastal landscapes: A review: The dynamic effects of sea level rise on low-gradient coastal landscapes. *Earth's Future*, *3*(6), 159–181. https://doi.org/10.1002/2015EF000298

Passeri, D. L., Hagen, S. C., Plant, N. G., Bilskie, M. V., Medeiros, S. C., & Alizad, K. (2016). Tidal hydrodynamics under future sea level rise and coastal morphology in the northern Gulf of Mexico: Tidal hydrodynamics under sea level rise. *Earth's Future*, *4*(5), 159–176. https://doi.org/10.1002/2015EF000332

Pawlowicz, R., Beardsley, B., & Lentz, S. (2002). Classical tidal harmonic analysis including error estimates in MATLAB using T_TIDE. *Computers & Geosciences*, *28*(8), 929–937. https://doi.org/10.1016/S0098-3004(02)00013-4

Pickering, M. D., Horsburgh, K. J., Blundell, J. R., Hirschi, J. J.-M., Nicholls, R. J., Verlaan, M., & Wells, N. C. (2017). The impact of future sea-level rise on the global tides. *Continental Shelf Research*, *142*, 50–68. https://doi.org/10.1016/j.csr.2017.02.004

Pickering, M. D., Wells, N. C., Horsburgh, K. J., & Green, J. A. M. (2012). The impact of future sea-level rise on the European Shelf tides. *Continental Shelf Research*, *35*, 1–15. https://doi.org/10.1016/j.csr.2011.11.011

Proudman, J. (1955a). The effect of friction on a progressive wave of tide and surge in an estuary. *Proceedings of the Royal Society of London. Series A. Mathematical and Physical Sciences*, *233*(1194), 407–418. https://doi.org/10.1098/rspa.1955.0276

Proudman, J. (1955b). The propagation of tide and surge in an estuary. *Proceedings of the Royal Society of London. Series A. Mathematical and Physical Sciences*, *231*(1184), 8–24. https://doi.org/10.1098/rspa.1955.0153

Pugh, D., & Woodworth, P. L. (2014). Sea-Level science: Understanding tides, surges, tsunamis and mean sea-level changes. https://doi.org/10.1017/CBO9781139235778

Rashid, M. M., Moftakhari, H., & Moradkhani, H. (2024). Stochastic simulation of storm surge extremes along the contiguous United States coastlines using the max-stable process. *Communications Earth & Environment*, *5*(1), 39. https://doi.org/10.1038/s43247-024-01206-z

Rashid, M. M., Wahl, T., & Chambers, D. P. (2021). Extreme sea level variability dominates coastal flood risk changes at decadal time scales. *Environmental Research Letters*, *16*(2), 24026. https://doi.org/10.1088/1748-9326/abd4aa

Rashid, M. M., Wahl, T., Chambers, D. P., Calafat, F. M., & Sweet, W. V. (2019). An extreme sea level indicator for the contiguous United States coastline. *Scientific Data*, *6*(1), 326. https://doi.org/10.1038/s41597-019-0333-x

Ray, R. D., & Foster, G. (2016). Future nuisance flooding at Boston caused by astronomical tides alone. *Earth's Future*, *4*(12), 578–587. https://doi.org/10.1002/2016EF000423

Ray, R. D., & Talke, S. A. (2019). Nineteenth-century tides in the Gulf of Maine and implications for secular trends. *Journal of Geophysical Research: Oceans*, *124*(10), 7046–7067. https://doi.org/10.1029/2019JC015277

Rossiter, J. R. (1961). Interaction between tide and surge in the Thames. *Geophysical Journal International*, *6*(1), 29–53. https://doi.org/10.1111/j.1365-246X.1961.tb02960.x

Santiago-Collazo, F. L., Bilskie, M. V., & Hagen, S. C. (2019). A comprehensive review of compound inundation models in low-gradient coastal watersheds. *Environmental Modelling & Software*, *119*, 166–181. https://doi.org/10.1016/j.envsoft.2019.06.002

Semedo, A., Sušelj, K., Rutgersson, A., & Sterl, A. (2011). A global view on the wind sea and swell climate and variability from ERA-40. *Journal of Climate*, *24*(5), 1461–1479. https://doi.org/10.1175/2010JCLI3718.1

Serafin, K. A., Ruggiero, P., & Stockdon, H. F. (2017). The relative contribution of waves, tides, and non-tidal residuals to extreme total water levels on US West Coast sandy beaches. *Geophysical Research Letters*, *44*(4), 1839–1847. https://doi.org/10.1002/2016GL071020

Street, J. O., Carroll, R. J., & Ruppert, D. (1988). A note on computing robust regression estimates via iteratively reweighted least squares. *The American Statistician*, *42*(2), 152. https://doi.org/10.2307/2684491

Sweet, W., Zervas, C., Gill, S., & Park, J. (2013). Hurricane Sandy inundation probabilities today and tomorrow. *Bull. Am. Meteorol. Soc*, *94*(9), S17–S20.

Sweet, W. V., Hamlington, B. D., Kopp, R. E., Weaver, C. P., Barnard, P. L., Bekaert, D., & Brooks (2022). *Global and regional sea level rise scenarios for the United States: Updated mean projections and extreme water level probabilities along U.S. Coastlines (No. NOAA techical report NOS 01)*. NOAA. Retrieved from https://oceanservice.noaa.gov/hazards/sealevelrise/noaa-nostechrpt01-global-regional-SLR-scenarios-US.pdf

Talke, S. A., & Jay, D. A. (2020). Changing tides: The role of natural and anthropogenic factors. *Annual Review of Marine Science*, *12*(1), 121–151. https://doi.org/10.1146/annurev-marine-010419-010727

Tebaldi, C., Ranasinghe, R., Vousdoukas, M., Rasmussen, D. J., Vega-Westhoff, B., Kirezci, E., et al. (2021). Extreme sea levels at different global warming levels. *Nature Climate Change*, *11*(9), 746–751. https://doi.org/10.1038/s41558-021-01127-1

Thompson, P. R., Widlansky, M. J., Hamlington, B. D., Merrifield, M. A., Marra, J. J., Mitchum, G. T., & Sweet, W. (2021). Rapid increases and extreme months in projections of United States high-tide flooding. *Nature Climate Change*, *11*(7), 584–590. https://doi.org/10.1038/s41558-021-01077-8

van Vuuren, D. P., Edmonds, J., Kainuma, M., Riahi, K., Thomson, A., Hibbard, K., et al. (2011). The representative concentration pathways: An overview. *Climatic Change*, *109*(1–2), 5–31. https://doi.org/10.1007/s10584-011-0148-z

Wahl, T. (2017). Sea-level rise and storm surges, relationship status: Complicated. *Environmental Research Letters*, *12*(11), 111001. https://doi.org/10.1088/1748-9326/aa8eba

Wahl, T., & Chambers, D. P. (2016). Climate controls multidecadal variability in U.S. extreme sea level records. *Journal of Geophysical Research: Oceans*, *121*(2), 1274–1290. https://doi.org/10.1002/2015JC011057

Wood, F. (1978). *Strategic role of Perigean spring tides in nautical history and North American coastal flooding, 1635–1976*. NOAA.

Woodworth, P. L. (2010). A survey of recent changes in the main components of the ocean tide. *Continental Shelf Research*, *30*(15), 1680–1691. https://doi.org/10.1016/j.csr.2010.07.002

Woodworth, P. L., Hunter, J. R., Marcos, M., Caldwell, P., Menéndez, M., & Haigh, I. (2016). Towards a global higher-frequency sea level dataset. *Geoscience Data Journal*, *3*(2), 50–59. https://doi.org/10.1002/gdj3.42

Woodworth, P. L., Melet, A., Marcos, M., Ray, R. D., Wöppelmann, G., Sasaki, Y. N., et al. (2019). Forcing factors affecting sea level changes at the coast. *Surveys in Geophysics*, *40*(6), 1351–1397. https://doi.org/10.1007/s10712-019-09531-1

Woodworth, P. L., Shaw, S. M., & Blackman, D. L. (2007). Secular trends in mean tidal range around the British Isles and along the adjacent European coastline. *Geophysical Journal International*, *104*(3), 593–609. https://doi.org/10.1111/j.1365-246X.1991.tb05704.x

Xiao, Z., Yang, Z., Wang, T., Sun, N., Wigmosta, M., & Judi, D. (2021). Characterizing the non-linear interactions between tide, storm surge, and river flow in the Delaware bay estuary, United States. *Frontiers in Marine Science*, *8*, 715557. https://doi.org/10.3389/fmars.2021.715557

Ye, F., Zhang, Y. J., Yu, H., Sun, W., Moghimi, S., Myers, E., et al. (2020). Simulating storm surge and compound flooding events with a creek-to-ocean model: Importance of baroclinic effects. *Ocean Modelling*, *145*, 101526. https://doi.org/10.1016/j.ocemod.2019.101526

Yim, S. C., Wei, Y., Azadbakht, M., Nimmala, S., & Potisuk, T. (2015). Case study for Tsunami design of coastal infrastructure: Spencer creek Bridge, Oregon. *Journal of Bridge Engineering*, *20*(1), 05014008. https://doi.org/10.1061/(ASCE)BE.1943-5592.0000631

Yu, C., & Yao, W. (2017). Robust linear regression: A review and comparison. *Communications in Statistics Simulation and Computation*, *46*(8), 6261–6282. https://doi.org/10.1080/03610918.2016.1202271

Zervas, C. (2013). *Extreme water levels of the United States 1893–2010 (No. technical report NOS CO-OPS 067)*. National Oceanic and Atmospheric Association. Retrieved from https://tidesandcurrents.noaa.gov/publications/NOAA_Technical_Report_NOS_COOPS_067a.pdf